Journal of Crystal Growth 470 (2017) 66–74

Contents lists available at ScienceDirect

Journal of Crystal Growth

journal homepage: www.elsevier.com/locate/crys

Dynamics of spacing adjustment and recovery mechanisms of ABAC-type growth pattern in ternary eutectic systems

Samira Mohagheghi, Melis Şerefoğlu *

Department of Mechanical Engineering, Koc University, Rumeli Feneri Yolu, 34450 Sariyer, Istanbul, Turkey

ARTICLE INFO

Article history:
Received 6 November 2016
Received in revised form 6 April 2017
Accepted 7 April 2017
Available online 8 April 2017
Communicated by T.F. Kuech

Keywords:
A1. Eutectics
A1. Solidification
A1. Directional solidification
A1. Optical microscopy
A2. Bridgman technique
B2. Alloys

ABSTRACT

In directionally solidified 2D samples at ternary eutectic compositions, the stable three-phase pattern is established to be lamellar structure with ABAC stacking, where A, B, and C are crystalline phases. Beyond the stability limits of the ABAC pattern, the system uses various spacing adjustment mechanisms to revert to the stable regime.

In this study, the dynamics of spacing adjustment and recovery mechanisms of isotropic ABAC patterns were investigated using three-phase In–Bi–Sn alloy. Unidirectional solidification experiments were performed on 23.0 and 62.7 μm-thick samples, where solidification front was monitored in real-time from both sides of the sample using a particular microscopy system. At these thicknesses, the pattern was found to be 2D during steady-state growth, *i.e.* both top and bottom microstructures were the same. However, during spacing adjustment and recovery mechanisms, 3D features were observed. Dynamics of two major instabilities, lamellae branching and elimination, were quantified. After these instabilities, two key ABAC pattern recovery mechanisms, namely, phase invasion and phase exchange processes, were identified and analyzed. After elimination, ABAC pattern is recovered by either continuous eliminations of all phases or by phase exchange. After branching, the recovery mechanisms are established to be phase invasion and phase exchange.

© 2017 Elsevier B.V. All rights reserved.

1. Introduction

The steady-state growth theory of two-phase regular eutectics was proposed by Jackson and Hunt (JH) in 1960s [1]. They proposed that the periodic lamellar structure grows close to the minimum undercooling spacing (λ_{JH}) at a given velocity and only stable within a limited eutectic spacing range. Beyond the stability regime, system undergoes catastrophic changes, namely, elimination and branching. Later, Akamatsu *et al.* showed that eutectics can grow below the minimum undercooling spacing due to phase diffusion phenomenon, which is the homogenization process of eutectic spacing distribution over time [2,3]. It is well established in the literature that, on the contrary to what JH proposed, branching does not take place in 2D samples [4–6]. In quasi-2D samples, however, branching does take place, as observed by JH but not with the mechanism that they proposed, *i.e.* nucleation of a new lamella in the negative curvature of branched lamella. JH theory still offers a reliable analytical method to study coupled growth of regular eutectics. The brief outcome of the theory is that the relationship between eutectic spacing corresponding to the minimum undercooling (λ_{JH}) and growth velocity (V) follows $\lambda_{JH}^2 V = K$, where K is a material constant.

In binary eutectic systems, the lamellar microstructure can only have the simplest configuration, *i.e.* AB, where A and B are crystalline phases present in the eutectic reaction. The stability diagrams of 2D lamellar eutectic structures with isotropic interfaces are well established for binary systems experimentally [5,7] and numerically [8]. At lower limit of stability diagram, the regime is bounded with elimination instability [4,7,8]. At upper limit, however, different types of instabilities have been observed; tilt bifurcation at off-eutectic compositions [5,8,9], period-preserving (1λO), period-doubling (2λO) oscillatory modes, and combination of them with the tilt state in 2D [5,8]; branching [1,4] and zigzag bifurcation in 3D samples [10,11]. These instabilities are all reported for the systems with isotropic solid/liquid (S/L) and solid/solid (S/S) interfacial energies. On the other hand, anisotropy of the S/S interfacial energy plays a significant role on the selection of microstructure [12–14].

In ternary eutectic systems, different microstructural configurations naturally exist due to the presence of three phases, *i.e.* A, B, and C. This adds complexity to the microstructure as well as the analysis of growth dynamics of three-phase systems, which are

* Corresponding author.
E-mail addresses: smohagheghi13@ku.edu.tr (S. Mohagheghi), mserefoglu@ku.edu.tr (M. Şerefoğlu).

http://dx.doi.org/10.1016/j.jcrysgro.2017.04.008
0022-0248/© 2017 Elsevier B.V. All rights reserved.

practically important class of alloys used in industry. In three-phase systems with isotropic S/L and S/S interfaces, among all other configurations, ABAC stacking (Fig. 1) was observed in different systems, including metals and organic materials [15–22]. The steadiness of ABAC pattern originates from the presence of mirror symmetry axes in the middle of B and C phases, which ease the solute redistribution in the solidification front during coupled growth [18,22,23]. Choudhury *et al.* studied the stability of this particular pattern numerically along with other configurations using phase-field method [23]. In a recent experimental study [22], stability of ABAC pattern was examined using In–Bi–Sn three-phase eutectic system, and the stability limits were determined for quasi-2D samples, where sample thickness was equal to 13 μm. Similar to two-phase systems, in three-phase eutectics, the lower and upper limits of the stability coincided with lamellae elimination and branching, respectively. ABAC pattern could be obtained after elimination and afterwards eutectic spacing profile was homogenized by phase-diffusion process. After branching, however, the symmetry was broken by formation of ABABAC-type patterns and thus phase diffusion phenomenon could not be verified after branching for three-phase eutectics. The details of these spacing adjustment mechanisms in three-phase systems are more complicated than the two-phase counterparts since, at the simplest case, a series of elimination or branching event should take place to preserve ABAC pattern. Alternatively, there may be some recovery mechanisms, which lead to ABAC growth pattern after these instabilities. Neither the dynamics of the spacing adjustment mechanisms nor the recovery mechanisms were determined or quantified yet.

In this study, directional solidification experiments with In–Bi–Sn three-phase eutectic system are performed to investigate the dynamics of the spacing adjustment and ABAC pattern recovery mechanisms in quasi-2D samples. Compared to 13 μm-thick samples, the confinement effect on the eutectic microstructure is observed to be less in our samples, which lead to more complex recovery mechanisms of ABAC pattern. The dynamics of these mechanisms are quantified by real-time observation of the solidification front from both sides of the sample using a particular microscopy system which we call double-sided microscope. Until now, real-time observation of the solidification front in metals could have been only done from one side of the sample, which is a huge disadvantage for metals compared to transparent organic systems used extensively in literature to understand the dynamics of solidification. This double-sided microscopy system overcomes the technical challenges created by metallic alloys and allows determination of the whole solidification front *in situ*.

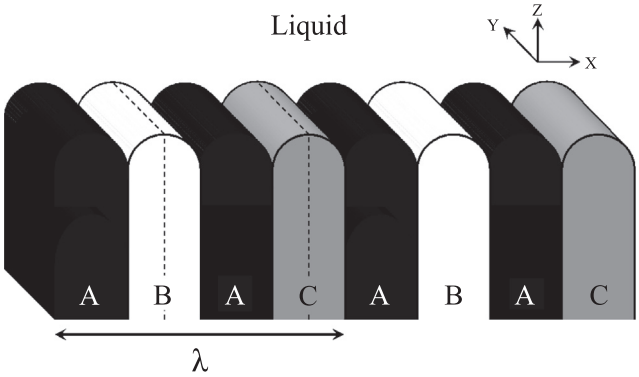

Fig. 1. Schematic representation of ABAC pattern during directional solidification. Mirror-symmetry planes at the center of B and C phases are shown with the dashed lines. λ is the eutectic spacing. Temperature is increasing in Z direction. Sample width and thickness are in X and Y directions, respectively.

2. Experimental procedure

In–Bi–Sn alloy close to the ternary eutectic point, which is at 60.2 at.% In–20.7 at.% Bi–19.1 at.% Sn, was prepared from 99.999% pure elements under Argon atmosphere. At ternary eutectic point (T_E = 59.2 °C), homogeneous liquid turns into three phases, namely In_2Bi, β-In, and γ-Sn [18,19,24], all of which have non-faceted solid/liquid interfaces. The composition of each phase is given in Table 1. The sample containers consist of two approximately 0.3 μm-thick glass plates separated by either 23 or 50 μm-thick Mylar spacers. Thickness of each glass plate was measured from three different locations and recorded. The samples were filled with the molten alloy by pressure and sealed right away to avoid contamination. The thicknesses of samples were also measured after filling. The thicknesses of the alloy samples, which were determined from the measured thickness values of glass plates and the total thickness after filling, are 23.0 μm and 62.7 μm for samples with 23 μm and 50 μm Mylar, respectively. We will use the actual sample alloy thickness values instead of Mylar thicknesses in the rest of the paper.

The samples were directionally solidified in a horizontal Bridgman-type setup at a fixed thermal gradient of 3.3 ± 0.1 K/mm. In brief, horizontal Bridgman setup consists of a hot and a cold zone made of copper blocks, and a motor to push the sample from hot to cold side in order to solidify it. While hot zone is heated by resistance heaters, water is circulated through the copper blocks of the cold zone. In order to avoid thermal fluctuations, which would destroy local equilibrium conditions, the sample is sandwiched between cold and hot blocks as shown in Fig. 2. This maximizes the contact surface of the blocks with the sample and minimizes the airflow. The blocks are fixed on an isolative plate with a gap in between and situated on top of the double-sided microscope stage, which enables real-time observation of solidification front from both top and bottom of the sample (Fig. 2). In this paper, top and bottom of the sample refers to the microstructure at the same XZ location on the sample observed using the top and bottom microscopes. The temperatures of hot and cold blocks are adjusted to place the solidification front in between zones. The investigated growth velocity range is 0.05–0.35 μm/s. During steady-state growth, the position of the S/L interface is stationary with respect to the laboratory frame. In other words, sample pushing velocity is equal to the growth velocity.

We use the typical eutectic spacing (λ) definition for three-phase eutectics in 2D, *i.e.* the width of one ABAC unit, as well as the Cartesian coordinates where Z, X, and Y are axes representing the direction of imposed thermal gradient, sample width, and sample thickness (δ), respectively (Fig. 1 and Fig. 2). The top and bottom microscope systems can be aligned such that both lenses are focused on the same region of the sample with a micrometer resolution. An example set of images showing ABAC pattern from top and bottom of the sample is given in Fig. 3. The microscopes are equipped with CMOS cameras, which are connected to computers for automated real-time acquisition of solidification front images. After contrast enhancement, each phase of the eutectic microstructure has a different color; that is, black (A), white (B), and gray (C) phases are In_2Bi, β-In, and γ-Sn, respectively.

Table 1
Composition of A, B, and C phases forming the eutectic microstructure [18].

Phase	In (at.%)	Bi (at.%)	Sn (at.%)
A: In_2Bi	66.48 ± 0.14	30.52 ± 0.23	3.00 ± 0.24
B: β-In	64.14 ± 0.42	11.38 ± 0.33	24.48 ± 0.27
C: γ-Sn	40.14 ± 0.21	16.11 ± 0.21	43.75 ± 0.35

Download English Version:

https://daneshyari.com/en/article/5489404

Download Persian Version:

https://daneshyari.com/article/5489404

Daneshyari.com